Nuclear Engineering and Technology 54 (2022) 860–866

Contents lists available at ScienceDirect

Nuclear Engineering and Technology

journal homepage: www.elsevier.com/locate/net

Original article

Numerical investigation on the hydraulic loss correlation of ring-type spacer grids

Kyung Ha Ryu [a, 1], Yong-Hoon Shin [b, 1], Jaehyun Cho [c, *], Jungho Hur [d], Tae Hyun Lee [a], Jong-Won Park [a], Jaeyeong Park [d], Bosik Kang [a]

[a] Department of Reliability Assessment, Mechanical System Safety Research Division, Korea Institute of Machinery and Materials, 156 Gajeongbuk-ro, Yuseong-gu, Daejeon, 34103, Republic of Korea
[b] Versatile Reactor Technology Development Division, Korea Atomic Energy Research Institute, 111, Daedeok-daero, 989 Beon-gil, Yuseong-gu, Daejeon, 34057, Republic of Korea
[c] Risk Assessment Research Team, Korea Atomic Energy Research Institute, 111, Daedeok-daero, 989 Beon-gil, Yuseong-gu, Daejeon, 34057, Republic of Korea
[d] School of Mechanical, Aerospace and Nuclear Engineering, Ulsan National Institute of Science and Technology, Ulju-gun, Ulsan, 44919, Republic of Korea

ARTICLE INFO

Article history:
Received 14 May 2021
Received in revised form
25 July 2021
Accepted 18 September 2021
Available online 27 September 2021

Keywords:
Ring-type spacer grid
Pressure drop
Drag coefficient
Lead-bismuth eutectic

ABSTRACT

An accurate prediction of the pressure drop along the flow paths is crucial in the design of advanced passive systems cooled by heavy liquid metal coolants. To date, a generic pressure drop correlation over spacer grids by Rehme has been applied extensively, which was obtained from substantial experimental data with multiple types of components. However, a few experimental studies have reported that the correlation may give large discrepancies. To provide a more reliable correlation for ring-type spacer grids, the current numerical study aims at figuring out the most critical factor among four hypothetical parameters, namely the flow area blockage ratio, number of fuel rods, type of fluid, and thickness of the spacer grid in the flow direction. Through a set of computational fluid dynamics simulations, we observed that the flow area blockage ratio dominantly influences the pressure loss characteristics, and thus its dependence should be more emphasized, whereas the other parameters have little impact. Hence, we suggest a new correlation for the drag coefficient as $C_B = C_{v,m}/\epsilon^{2.7}$, where $C_{v,m}$ is formulated by a nonlinear fit of simulation data such that $C_{v,m} = -11.33\ \ln(0.02\ \ln(\mathrm{Re}_b))$.

1. Introduction

Lead alloys such as pure lead and lead–bismuth eutectic (LBE) are evaluated as promising coolants for next-generation reactors. They feature high boiling points, chemical inertness to air and water, and low neutron absorption, enabling a simpler primary system design and safer operation under a fast neutron spectrum. Taking advantage of these favorable features, research and development of lead- or LBE-cooled fast reactors (LFRs) has progressed in a relatively short period compared to systems adopting other novel coolants, mainly due to their ease of use. This progress is evidenced in a report from the Generation IV International Forum in 2014 stating that LFRs are anticipated to be deployed earlier than the other five new reactor types [1].

Despite the bright prospects, lead alloys have faced a common challenge in terms of material compatibility with other structural materials given by their corrosive natures, and likewise, concerns about erosion in conjunction with their high densities. For this reason, most LFR designs have empirically set the maximum flow velocity to 2–3 m/s and arranged the flow channels in the core in a large lattice, which aggravates neutron economy in fast neutron spectra. Furthermore, this limitation affects thermal-hydraulic designs, leading to a lower power density and making them less economically competitive compared to their main competitor, the sodium-cooled fast reactor (SFR).

Despite this, open lattice arrangements of the flow channels in the core could be beneficial in fast reactors in cases where the reactor design does not require a high power density. Compared to SFRs, LFRs can achieve a high pitch-to-diameter ratio since they are rather free from positive reactivity insertion given by void formation [2]. With a large open lattice, wire wrappers, which are widely used and have been considered as the first option for SFR fuel bundles, do not have to be applied, a point that also contributes to a

* Corresponding author.
E-mail address: chojh@kaeri.re.kr (J. Cho).
[1] Contributed equally to this manuscript (Kyung Ha Ryu, Yong-Hoon Shin).

https://doi.org/10.1016/j.net.2021.09.019

Nomenclature

ΔP	Pressure loss (Pa)
A	Area (m^2)
C_B	Drag coefficient across a spacer grid
C_v	Modified drag coefficient
D	Diameter (m)
L	Length of flow development (m)
$\dot{m}$	Mass flow rate (kg/s)
Re	Reynolds number
T	Temperature (K)
w	Flow speed (m/s)
Greek letters	
ε	Flow area blockage ratio ($= A_{grid}/A_b$)
μ	Dynamic viscosity (Pa s)
ρ	Fluid density (kg/m^3)
Subscripts	
b	Fuel bundle
grid	Spacer grid
h	Hydraulic
LBE	Lead-bismuth eutectic
m	Modified in this study
max	Maximum

lower pressure loss through the core, thereby enhancing the natural circulation capability of the system. In accident conditions when the reactor may not rely on reactor coolant pumps, this guarantees core cool ability for an extended period, which aligns well with the Generation IV reactor design philosophy. Several LFR concepts have thus tried to make use of this favorable feature with large core lattices, depending entirely on natural circulation for system cooling even in normal operation [3–6]. In these cases, the fuel rods are tied to some spacer grids in common. Spacer grids, accordingly, are of special interest in passive LFRs, for which the total hydraulic loss should be accurately estimated since both temperature distribution and coolant mass flow are strongly coupled to the parameter. Considering the compactness of fuel rods in the core, pressure loss across a spacer grid is expected to have the greatest influence on the total hydraulic loss [7,8].

In general, the pressure drop across a spacer grid is able to be correlated to the dynamic pressure upstream of the component where the flow has not yet been disturbed with a proportionality constant called the drag coefficient, C_B, such that

$$\Delta P_{grid} = C_B \frac{1}{2} \rho w_B^2 \tag{1}$$

in which the bundle fluid velocity, w_b, is utilized as the dynamic pressure term. Up to now, a pioneering experimental study on various kinds of spacer grids by Rehme provided numerous data to characterize C_B, which was aimed to be used for fast breeder reactors with the tests conducted under water [9]. It was figured out that the term has a strong dependence on the flow area blockage ratio, ε, which is defined as $\varepsilon = A_{grid}/A_b$, so that it can be expressed with another term called the modified drag coefficient, C_v, such that

$$C_B = C_v \varepsilon^2 \tag{2}$$

The work by Rehme originally indicated that C_v is given as $C_v = 6–7$ for $Re_b > 5 \times 10^4$, without providing a correlation for low-Re flow conditions. As a complementary work, Cigarini and Dalle Donne suggested an empirical correlation based on Rehme's experimental data in their analytical study [10] as

$$C_v = 3.5 + \frac{73.14}{Re_b^{0.264}} + \frac{2.79 \times 10^{10}}{Re_b^{2.79}} \tag{3}$$

Here, if C_v is given such that $C_B > 2$, then the parameter is limited by $C_v = 2/\varepsilon^2$ so that C_B does not exceed $C_B = 2$.

However, it has been reported from several experimental activities that the Rehme correlation shows a large discrepancy. Yao et al. compared their single-phase experimental data to the Rehme correlation and found that a 50% higher correction to the loss coefficient appeared to be more appropriate [11]. Schikorr et al. adjusted the flow blockage ratio from $\varepsilon = 0.355$ to $\varepsilon = 0.4757$ accompanied by a modification of the maximum value of C_B to 2.6 instead of 2 to obtain good agreement between their code calculation and experimental data [12]. They were not able to justify the adjustment of ε, though, since the original value was estimated from the actual dimensions of spacer grids. Cho et al. also reported that the measured pressure loss in a component in a loop containing a couple of identical ring-type spacer grids cannot be predicted by the Rehme correlation, which led to an ad hoc modification of C_v to match their experimental data to their code calculation [7].

In this regard, the current study suggests a new correlation for the pressure drop that can give a more reliable prediction for ring-type spacer grids in passive LBE systems through computational fluid dynamics (CFD) modeling. In Section 2, the spacer grids of interest are selected, and the computational domains are defined so that a case study on various factors can be conducted. In this regard, we identified such parameters that can affect the pressure drop across a ring-type spacer grid: the number of rods in the fuel bundle, the dimensions of the spacer grid represented by ε and its thickness in the traversing direction, and the type of coolant. For characterization, a number of CFD simulations were conducted over three different arrangements of ring-type spacer grids under various flow conditions in the range $3 \times 10^3 < Re_b < 10^5$. The simulation results are compared in Section 3 in terms of C_B and C_v. As a result, a new correlation of C_B is suggested, accompanied by a more generic formulation of C_v obtained from a nonlinear fitting of the simulated data.

2. Modeling approach

2.1. Spacer grid models

The C_B for ring-type spacer grids was originally suggested as function of Re_b and ε, as in Equations (2) and (3). However, the discrepancies reported in the literature indicate that other parameters should be taken into account as well to estimate the pressure loss. To investigate further into the pressure drop characteristics over the components, we selected several additional factors that might also affect the flow behavior, namely the number of rods, type of coolant, and thickness of the spacer grid, in addition to ε.

First of all, the number of rods could be crucial as it directly relates to the flow distribution and separation across the subchannels even if ε is given to be the same in different arrangements. As the number of rods increases, the internal flow channels eventually outnumber the side channels and become dominant, which in turn suggests that the importance of the lateral flow decreases. In this regard, a 2×2 rod arrangement identical to the HELIOS spacer grid [7] was chosen as the baseline, and 3×3 and 4×4 lattices

were included in the analytical models. All have structured and symmetric layouts, while the dimensions of the enclosing flow paths, which are given to be pipe flows, are determined so that the bare flow area ratios are similar to each other under the same rod diameter of 12.7 mm and pitch-to-diameter ratio of 1.38.

In terms of coolant, since the study mainly focuses on a correlation intended for use in LBE environments, most of the simulations were conducted with LBE properties except one case with those of water. Another impact can be given by the thickness of the grid. With the same rationale as the HELIOS spacer grid being the baseline, most of the cases were defined with a thickness of 5 mm in the flow direction, with one 10 mm case. Variation in ε can be achieved by changing the thickness of the constituent elements such as the inner rings that grip the rods and the outer rings that support the position of the spacer grid itself.

The above considerations led us to define seven different kinds of ring-type spacer grids, as summarized in Table 1. The modeled ring-type spacer grids in 2 × 2, 3 × 3, and 4 × 4 arrangements are depicted in Fig. 1, where only one representative design is shown for the 3 × 3 type.

2.2. Computational domain setup and solver settings

The computational domains in different grids contain three regions each, namely the upstream, spacer, and downstream regions, as shown in Fig. 2. The upstream regions were required to be long enough to guarantee that the flow arriving at the grid is fully developed and to minimize numerical errors that might be generated by an ill-conditioned geometry. For the minimum length under a given flow condition, the following relation can be used,

$$4.4\mathrm{Re}_b^{1/6} = \frac{L}{D_h} \tag{4}$$

with which the domain lengths were given to be longer than L. On the other hand, the downstream domains were made to be at least five times longer than D_h.

The fluid domains were discretized by ICEM-CFD as shown in Fig. 3. The upstream and downstream regions were meshed dominantly with hexahedral elements, while tetrahedral cells were mainly used in the grid regions. To capture the near-wall flow behavior, a few inflation layers were included where applicable. The analytic models assumed 250 °C for the LBE models and 25 °C for the sole water model, and isothermal conditions were given to the domain boundaries. The inlets were set to be the mass sources where the fluid flow starts with flow rates up to 30 kg/s, ranging over $3 \times 10^3 < \mathrm{Re}_b < 10^5$.

The simulations were conducted with Ansys CFX using the k-ε turbulence model with the scalable wall function for the solution process as the use of the model for a similar flow condition was shown to be reliable [7]. The turbulent Prandtl number was set to be 2, which is in conjunction with the best practice guidelines for liquid metal CFD [13]. The properties of LBE were taken from the LBE handbook by OECD/NEA [14], while the water case calculation was done with the material properties provided by the software package at the designated temperatures.

3. Results and discussion

3.1. Drag coefficient (C_B)

The pressure loss characteristics over different ring-type spacer grids defined in Section 2.1 can be represented by C_B. All the simulation results at different flow conditions are shown in Fig. 4 in terms of C_B, which were obtained from Equation (1) by dividing the pressure loss by the upstream dynamic pressure ($\rho w_b^2/2$). The discrete data points are compared with the solid lines derived from Equation (3) at $\varepsilon = 0.232$, 0.373, and 0.482, while the dashed horizontal lines indicate that the correlation is given to be lower than a maximum of $C_{B,\max} = 2$ from the original Rehme's correlation [9], and $C_{B,\max} = 2.6$ in case of the suggestion by Schikorr et al. [12], as summarized in Section 1. The values of ε used for the curves were chosen to be close to those of the spacer grid models used in this study.

It can be confirmed from Fig. 4 that the number of rods and their arrangements, the type of coolant, and the thickness of the spacer grid do not significantly affect the pressure loss characteristics, as the cases with ε ~0.48, all of which are parametrized by those selected aspects, converge to each other closely. However, the spread with respect to C_B at a given Re_b indicates that the hydraulic loss definitely depends on ε, which also supports the previous observations in the literature so far. The larger the flow area blockage ratio, the larger the pressure drop, a trend evidencing that ε has a more important role than other parameters in the hydraulic loss over a ring-type spacer grid.

In addition, it can be seen that the Rehme correlation is still valid for two types of 3 × 3 grids with $\varepsilon = 0.232$ and $\varepsilon = 0.373$, as the solid lines with the same ε values have little discrepancy with the simulation results except for the cases at low flow rates around $\mathrm{Re}_b = 3 \times 10^3$. Originally, experimental data from only one type of ring-type spacer grid at $\varepsilon = 0.203$ was utilized, while the correlation was drawn out from many different geometries of spacer grids [9]. This fact may suggest that the validity of the correlation can be confirmed by the simulation results in particular for the ring-type

Table 1
Geometrical parameters of the spacer grids modeled in this study.

Parameter	Grid type						
Rod bundle arrangement	2 × 2	3 × 3	3 × 3	3 × 3	3 × 3	3 × 3	4 × 4
Pipe inner diameter (mm)	49.5	74.5	74.5	74.5	74.5	74.5	107.5
Rod diameter (mm)	12.7	12.7	12.7	12.7	12.7	12.7	12.7
Pitch-to-diameter ratio	1.38	1.38	1.38	1.38	1.38	1.38	1.38
Number of rods	4	9	9	9	9	9	16
Undisturbed flow area in rod bundle (cm^2)	14.18	32.19	32.19	32.19	32.19	32.19	70.49
Upstream length for flow development at Re = 10^5 (m)	1.49	2.24	2.24	2.24	2.24	2.24	3.23
Fluid*	LBE	LBE	LBE	Water	LBE	LBE	LBE
Spacer grid support ring diameter (mm)	45.5	68.4	68.4	68.4	69.6	71.7	96
Spacer grid ring diameter (mm)	16.7	16.7	16.7	16.7	15.7	14.7	16.7
Spacer grid ring thickness (mm)	2.0	2.0	2.0	2.0	1.5	1.0	2.0
Plugging area (cm^2)	6.91	15.37	15.37	15.37	12.02	7.46	33.57
Grid thickness (mm)	5.0	5.0	10.0	5.0	5.0	5.0	5.0
Flow area blockage ratio	0.487	0.477	0.477	0.477	0.373	0.232	0.476

* For LBE simulation, the thermophysical properties at $T = 250$ °C were used, while those of water were taken at $T = 25$ °C.

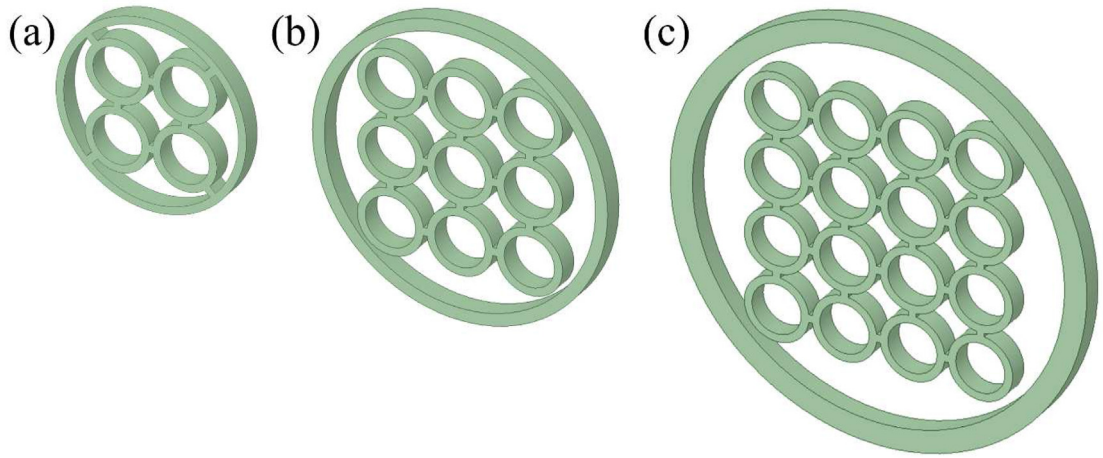

Fig. 1. Spacer grid types of (a) 2 × 2, (b) 3 × 3, and (c) 4 × 4 modeled in this study. Note that only one type of grid is represented in (b) among several variations of the 3 × 3-type grids defined in Table 1.

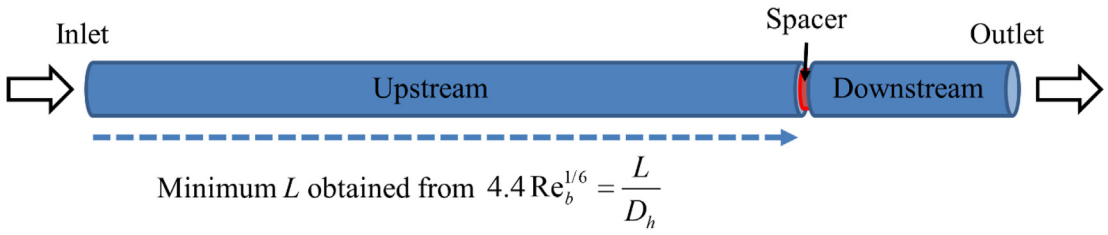

Fig. 2. Schematic representation of the computational domain with a spacer grid.

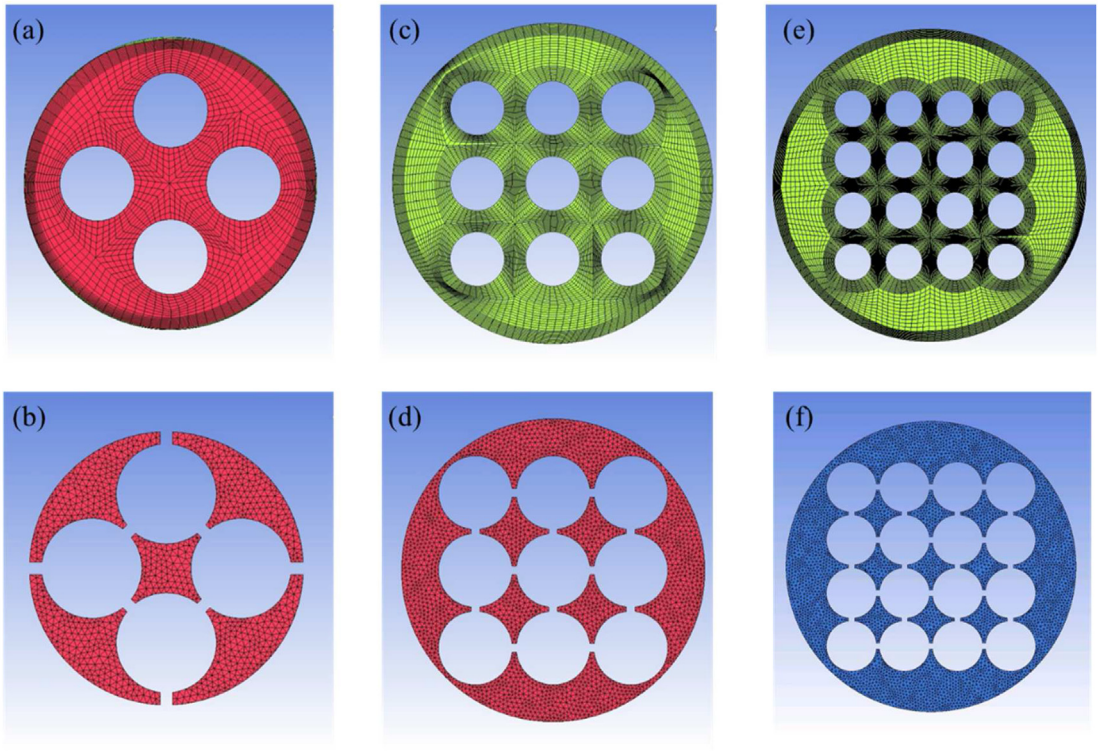

Fig. 3. Fluid domain meshes generated on the bare flow regions [(a), (c), and (e)] and grid regions [(b), (d), and (f)] for 2 × 2-type, 3 × 3-type, and 4 × 4-type arrangements, respectively.

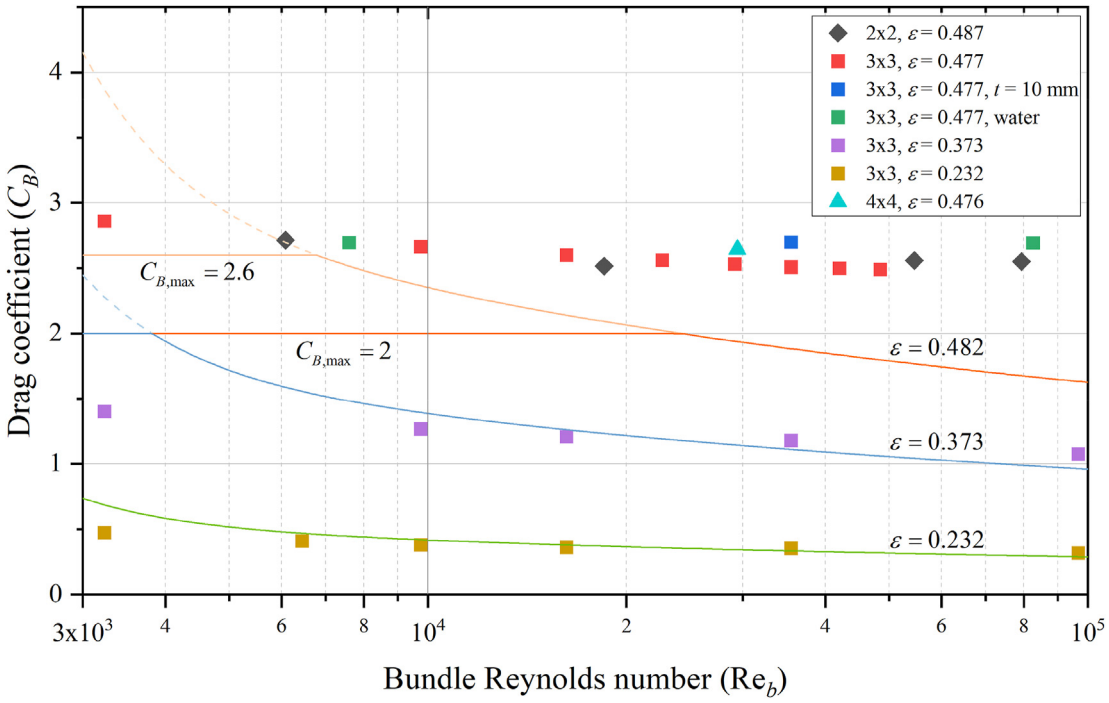

Fig. 4. Simulation results represented by the drag coefficient (C_B) as a function of bundle Reynolds number (Re_b). The solid curves are Equation (3) [10] at different flow blockage ratios of $\varepsilon = 0.232$, 0.373, and 0.482. The dashed curves are extensions of the equation unless clipped by $C_{B,max}$, which was originally suggested as $C_{B,max} = 2$ [9], while a modification, $C_{B,max} = 2.6$, was applied so that the correlation is valid [12].

spacer grids with a similar flow area blockage ratio and could be extended up to $\varepsilon = 0.373$.

However, the correlation is not able to be applied to the cases with higher ε values such as from $\varepsilon = 0.476$ to $\varepsilon = 0.487$, as can be seen in the simulation results. Furthermore, the modified correlation [12] cannot be used either, since it is merely a selective correction to the low-flow regime values so that a higher value of C_B may be rendered. In all the investigated flow conditions, both correlations underestimate the pressure loss over the component at around $\varepsilon = 0.48$. This underestimation is also thought to be a common conclusion from the previous experimental activities in the literature regardless of the shape or type of spacer grid.

3.2. Modified drag coefficient (C_v)

The comparison between the correlation and simulation results summarized in Section 3.1 led us to a further investigation on C_v. Applying Equation (2), Fig. 5 illustrates the simulation results reformulated as $C_v = C_B/\varepsilon^2$. Since the dependence in ε should no longer appear in the relation, all the results should converge to a single curve if the original relation, Equation (3), is valid for the range $0.24 < \varepsilon < 0.48$. However, it is rather clearly pronounced that the results spread with respect to discrete ε values in Fig. 5. This distribution strongly implies that the dependence of the pressure drop on ε is higher than the second-order dependence reported by Rehme.

The large deviations might be due to the fact that the original correlation was drawn from a wide range of data including various geometrical shapes. Although the general characteristics of pressure loss over different shapes could be represented by ε, the same level of discrepancy in a given type of grid at different ε cannot be guaranteed. Considering though that C_B is proportional to ε^2 in Equation (2), discrepancies in C_v at low values of ε such as $\varepsilon = 0.24$ can be well managed. But the higher ε becomes, the less the discrepancy can be neglected. Hence, for a reliable estimation of pressure loss across a ring-type spacer grid, ε, a novel correlation that is able to encompass a large range of ε is necessary.

3.3. Suggestion of a new pressure loss correlation

This section is dedicated to the suggestion of a new correlation not only for C_B but also for C_v, as we have identified that the pressure loss characteristics of ring-type spacer grids should be more dependent on ε. A realistic approach would be to account for the strong dependence on ε by means of a higher exponent in Equation (2) such that the new C_v relation given in this study falls onto a single curve regardless of the value of ε. By trial-and-error, we were able to find out that an exponent of 2.7 works well in eliminating the dependence of ε from C_v, and thus we suggest

$$C_B = C_{v,m}\varepsilon^{2.7} \tag{5}$$

as a new C_B correlation. Within this convention, Equation (1) can be used with no further adaptation. By applying Equation (5) to the simulation results, all the data points can be drawn over in Fig. 6, which indicates $C_{v,m}$ is solely given as a function of Re_b. Since the exponent was revised, Equation (3) is no longer valid; thus, we provide a new formulation obtained from a nonlinear fitting using the Bradley model, to make the correlation as simple as possible while keeping its accuracy,

$$C_{v,m} = -11.33\ln(0.02\ln Re_b) \tag{6}$$

which is drawn in Fig. 6 as well. The maximum error from the relation to the data points was estimated to be 6%, suggesting that Equations (5) and (6) are applicable over a large range of ε from around $\varepsilon = 0.2$ to $\varepsilon = 0.5$.

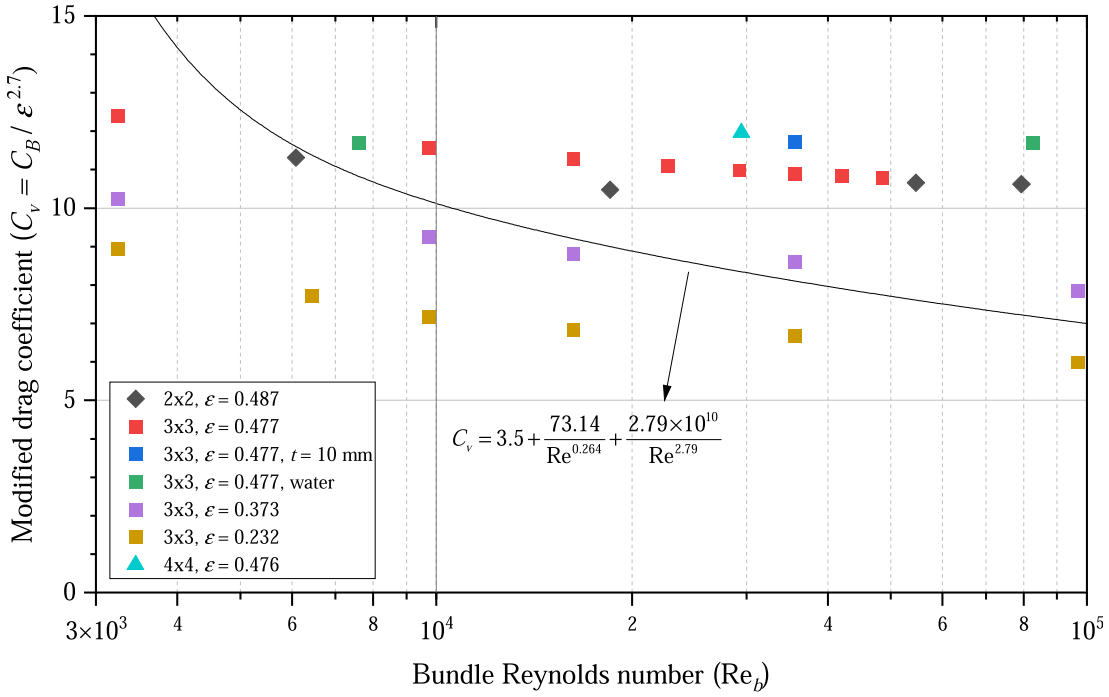

Fig. 5. Simulation results represented by the modified drag coefficient (C_v) in accordance with Equation (2) as a function of bundle Reynolds number (Re_b). The solid curve follows Equation (3) [10], while the data points not converging to the curve indicate that the dependence on the flow area blockage ratio (*&epsi*) still remains.

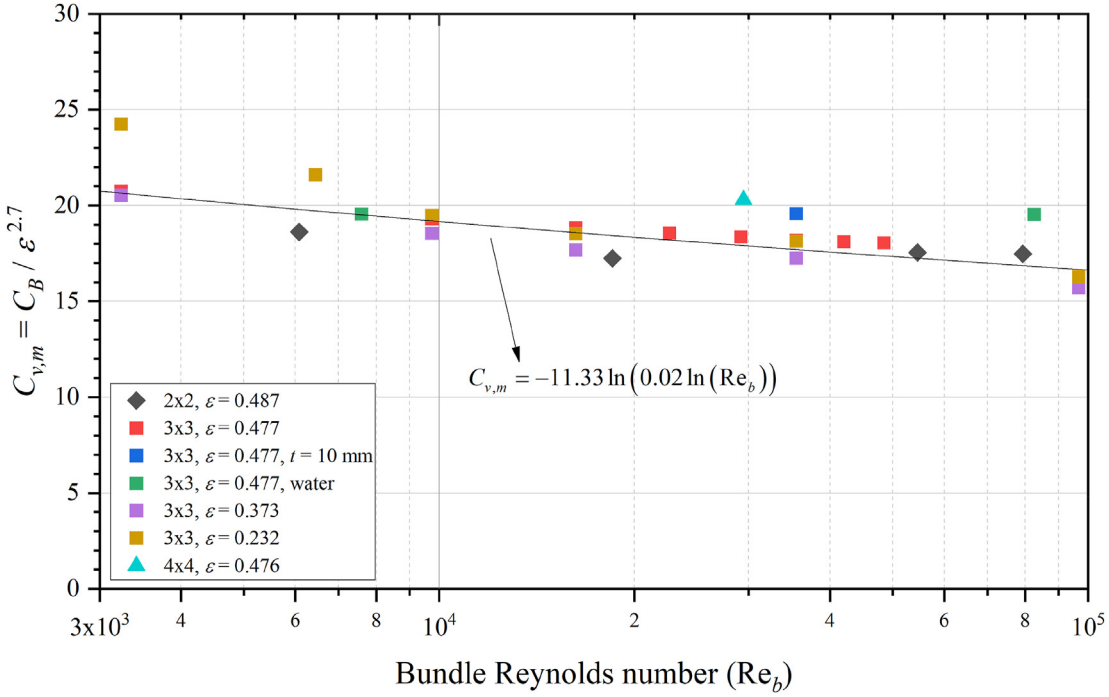

Fig. 6. Simulation results with respect to Equation (5) as a function of bundle Reynolds number (Re_b). The solid line is the new correlation obtained from nonlinear fitting.

4. Conclusions

Lead and LBE have been regarded as promising coolants for advanced passive reactor systems thanks to their favorable natures. As the design parameters of such systems are strongly coupled with each other, pressure loss correlations are the most important ones to be provided with guaranteed accuracy since the total pressure loss along the flow paths determines the temperature distribution and mass flow rate passively. Simultaneously, pressure loss should be minimized to ensure a higher natural circulation flow rate to lower the core outlet temperature and to ensure the cooling capacity of the reactor core in adverse conditions. To achieve this, the core should be equipped with fuel assemblies having large flow areas and minimal flow restrictions, which contribute to a lower

pressure drop across the components.

In this respect, spacer grids can be employed owing to their simple geometries in comparison to the wire wrappers that have traditionally been used in SFR fuel bundles. So far, a generic pressure loss correlation for spacer grids based on extensive experimental work reported by Rehme in the 1970s and its slight revisions in accordance with different types of grids have been applied to the prediction of pressure loss characteristics over such components, especially in liquid metal reactor applications. However, some experimental studies have pointed out that the correlation is limited and does not account for geometrical parameters precisely.

Motivated by the observations in the literature, we proposed a more reliable correlation for ring-type spacer grids in LBE through numerical investigation. We conducted a number of simulations on pressure drop across three different types of ring-type spacer grids over a wide range of flow velocities in isothermal conditions considering different factors that might influence the hydraulic loss characteristics. Through the CFD analyses, it was confirmed that the extent of flow area blockage by the grid is the most important factor determining the pressure loss.

We figured out that the conventional correlation for spacer grids, which is a generic formulation given by an extensive amount of experimental data from various types of grids, shows a large discrepancy if used for a grid with a large flow area blockage ratio, ε. Based on the numerical modeling results, a new model was presented first by updating the exponent given to the factor from 2 to 2.7 as determined by trial-and-error to take the strong dependence of pressure loss in ε into account. The implementation also led to a suggestion for an additional correlation of the so-called the modified drag coefficient, C_v. The correlation was drawn from a nonlinear fitting of the simulation data and given as a function of bundle Reynolds number, Re_b, showing reliable results with a maximum error of 6%. Owing to its simple form and wide range of application, we also expect that this correlation allows nuclear system designers to streamline the design of passive pumpless nuclear systems without extra efforts to obtain realistic design values.

Declaration of competing interest

The authors declare that they have no known competing financial interests or personal relationships that could have appeared to influence the work reported in this paper.

Acknowledgments

This work was supported by the Mass Production Performance Assessment Program (1415171778), the Materials & Components Technology Development Program (1415171720, 1415171728), the Technology Innovation Program (20011164), and the Energy Technology Development Program (20215810100050) funded by the Korean Government Ministry of Trade, Industry and Energy.

References

[1] Generation IV International Forum, Technology Roadmap Update for Generation IV Nuclear Energy Systems, OECD Nuclear Energy Agency, Paris, France, 2014.
[2] K. Tuček, J. Carlsson, H. Wider, Comparison of sodium and lead-cooled fast reactors regarding reactor physics aspects, severe safety and economical issues, Nucl. Eng. Des. 236 (2006) 1589–1598, https://doi.org/10.1016/j.nucengdes.2006.04.019.
[3] S. Choi, J.-H. Cho, M.-H. Bae, J. Lim, D. Puspitarini, J.H. Jeun, H.-G. Joo, I.S. Hwang, PASCAR: long burning small modular reactor based on natural circulation, Nucl. Eng. Des. 241 (2011) 1486–1499, https://doi.org/10.1016/j.nucengdes.2011.03.005.
[4] Y.-H. Shin, S. Choi, J. Cho, J.H. Kim, I.S. Hwang, Advanced passive design of small modular reactor cooled by heavy liquid metal natural circulation, Prog. Nucl. Energy 83 (2015) 433–442, https://doi.org/10.1016/j.pnucene.2015.01.002.
[5] J.J. Sienicki, B.W. Spencer, Power optimization in the STAR-LM modular natural convection reactor system, American Society of Mechanical Engineers Digital Collection, 2009, pp. 685–690, https://doi.org/10.1115/ICONE10-22294.
[6] D.C. Wade, E. Feldman, J. Sienicki, T. Sofu, A. Barak, E. Greenspan, D. Saphier, N.W. Brown, Q. Hossain, M.D. Carelli, L. Conway, M. Dzodzo, ENHS: the encapsulated nuclear heat source — a nuclear Energy concept for emerging worldwide Energy markets, American Society of Mechanical Engineers Digital Collection, 2009, pp. 583–590, https://doi.org/10.1115/ICONE10-22202.
[7] J.H. Cho, A. Batta, V. Casamassima, X. Cheng, Y.J. Choi, I.S. Hwang, J. Lim, P. Meloni, F.S. Nitti, V. Dedul, V. Kuznetsov, O. Komlev, W. Jaeger, A. Sedov, J.H. Kim, D. Puspitarini, Benchmarking of thermal hydraulic loop models for Lead-Alloy Cooled Advanced Nuclear Energy System (LACANES), phase-I: isothermal steady state forced convection, J. Nucl. Mater. 415 (2011) 404–414, https://doi.org/10.1016/j.jnucmat.2011.04.043.
[8] A. Batta, J. Cho, A. Class, I. Hwang, CFD analysis of heavy liquid metal flow in the core of the HELIOS loop, Nuclear Engineering and Technology (2010) 42, https://doi.org/10.5516/NET.2010.42.6.656.
[9] K. Rehme, Pressure drop correlations for fuel element spacers, Nucl. Technol. 17 (1973) 15–23, https://doi.org/10.13182/NT73-A31250.
[10] M. Cigarini, M. Dalle Donne, Thermohydraulic optimization of homogeneous and heterogeneous advanced pressurized water reactors, Nucl. Technol. 80 (1988) 107–132, https://doi.org/10.13182/NT88-A35553.
[11] S.C. Yao, L.E. Hochreiter, W.J. Leech, Heat-transfer augmentation in rod bundles near grid spacers, J. Heat Tran. 104 (1982) 76–81, https://doi.org/10.1115/1.3245071.
[12] M. Schikorr, E. Bubelis, L. Mansani, K. Litfin, Proposal for pressure drop prediction for a fuel bundle with grid spacers using Rehme pressure drop correlations, Nucl. Eng. Des. 240 (2010) 1830–1842, https://doi.org/10.1016/j.nucengdes.2010.03.039.
[13] F. Roelofs (Ed.), Thermal Hydraulics Aspects of Liquid Metal Cooled Nuclear Reactors, Elsevier, 2019, https://doi.org/10.1016/C2016-0-01216-0.
[14] OECD Nuclear Energy Agency, Handbook on Lead-bismuth Eutectic Alloy and Lead Properties, Materials Compatibility, Thermal-hydraulics and Technologies, 2015 edition, OECD Nuclear Energy Agency, Paris, France, 2015.